Crystallization and Structure Determination of s3-Form II from ColH: The second form of s3 crystals were obtained by hanging drop vapor diffusion from 1.1-1.4 M sodium acetate, 0.1 M HEPES (pH 7.5), 1 mM $CaCl_2$ and 0.05 M $CdSO_4$. The crystals were flash frozen in liquid nitrogen without the need of additional cryoprotectant. This crystal form of s3 diffracted to 2.2Å resolution and was isomorphous to the first form. We were planning to solve s3 structure by single isomorphous replacement method. Ca^{2+} ions and solvent molecules were deleted from the ColH model described above before refinement using REFMAC. The size of F_o-F_c difference peaks indicated that 12 of them are of cations. Two cations per molecule were geometrically identical to Ca^{2+} bound to s3b and those of s3 in the form I. Six peaks were therefore assigned as Ca^{2+}. Later it became clear that the B-factor of one of the two Ca^{2+} was too low (<5 $Å^2$). It was therefore reassigned as Cd^{2+}. The rest of the strong F_o-F_c difference peaks were assigned as Cd^{2+} ions. Two Cd^{2+} ions are chelated with surface glutamic acids (Glu876 and Glu930), respectively in each of the three molecules. The main-chain (C_α) root mean square deviation between Form I and Form II was only 0.35Å.

Tables

Supplementary Table 1. Data collection and refinement statistics

	Holo-s3 Form II
Data collection statistics (a)	
Wavelength (Å)	0.97937
Space group	$P2_12_12_1$
a, b, c (Å)	61.6,64.6, 96.0
beta(°)	90.0
Unique Reflections	19,933
d_{min} (Å) (b)	28.68-2.20
Completeness (%) (c)	98.8 (99.7)
I/σI (b)	9.6 (2.4)
R_{meas} (%) (d)	17.9 (66.4)
Redundancies	3.6 (3.4)

Refinement Statistics	
Resolution (Å)	28.68-2.20
R-factor (%)	17.6 (20.4)
R_{free} (%) 10% of data	25.0 (27.2)
Average B-factor main chain in A (A^2)	19.6
Average B-factor side chain in A (A^2)	21.7
Average B-factor main chain B (A^2)	18.3
Average B-factor side chain B (A^2)	20.5
Average B-factor main chain C (A^2)	19.4
Average B-factor side chain C (A^2)	22.0
RMS Deviations from restraint target values	
Bond Lengths (Å)	0.02
Bond Angles (°)	1.9
Distances form Restraint Planes	0.008
Ramachandran Statistics	
Most favorable (%)	91.0
Additionally allowed (%)	9.0
Disallowed (%)	0.0

(a) For more complete data collection statistics, see Supplementary Table 9.

(b) Highest resolution shell for holo-s3 form II: 2.24-2.20 Å

(c) Data for the highest resolution shell are given in parenthesis

(d) $R_{meas} = \sum_h \sqrt{\frac{n_h}{n_{h-1}}} \sum_l |I_{hl} - \langle I_h \rangle| / \sum_h \sum_l \langle I_h \rangle$

Supplementary Table 2. Calcium-oxygen atom distances and deviation from planarity in pentagonal bipyramid coordination.

s3b	Residue	E901	E901	D904	R929	D930	N903, axial	D927, axial	
	Atom	OE1	OE2	OD2	O	OD1	OD1	OD1	Ca^{2+}
Oxygen-calcium distances (Å) (a)	Average of Molecules A and B	2.56 (2)	2.41 (1)	2.34 (2)	2.36 (1)	2.35 (2)	2.35 (1)	2.43 (2)	3.75 (1)
Distance out of equatorial LSQ plane (Å) (ab)	Average of Molecules A and B	0.29	0.32	0.21	0.19	0.15	NA	NA	0.05
s3-Form I	Residue	E870	E870	N873	Q898	D899	N872	D897	
	Atom	OE1	OE2	OD1	O	OD1	OD1	OD1	Ca^{2+}
Oxygen-calcium distances (Å)	Average of Molecules A, B and C	2.56 (6)	2.45 (3)	2.34 (5)	2.39 (1)	2.38 (4)	2.34 (5)	2.28 (2)	3.77 (2)
Distance out of equatorial LSQ plane (Å) (ab)	Average of Molecules A, B and C	0.34 (5)	0.28 (9)	0.27 (12)	0.24 (8)	0.12 (6)	NA	NA	0.06 (4)
s3-Form II	Residue	E870	E870	N873	Q898	D899	N872	D897	
	Atom	OE1	OE2	OD1	O	OD1	OD1	OD1	Ca^{2+}
Oxygen-calcium distances (Å)	Average of Molecules A, B and C	2.62 (4)	2.55 (10)	2.37 (5)	2.35 (6)	2.40 (4)	2.34 (5)	2.30 (1)	3.66 (3)

A number within parenthesis represents an estimated standard deviation obtained after least square refinement (2.54 (2) means 2.54±0.02 Å). Measurements are for the distance of specific atom out of the plane created by the five members and do not include the axial members. Additionally, the distance of calcium from each plane was also calculated.

Supplementary Table 3: Calcium- oxygen atom distances and deviation from planarity in square antiprismatic coordination.

s3b	Residue	E899	E899	E901	H_2O		S922	D927	D930	D930
	Atom	OE1	OE2	OE2	O	Ca^{2+}	O	OD2	OD1	OD2
Oxygen-calcium distances (Å) (a)	Average of Molecules A and B	2.51 (2)	2.46 (1)	2.36 (2)	2.44	3.75 (1)	2.32 (2)	2.41 (2)	2.47 (1)	2.60 (2)
Distance out of square LSQ plane (Å) (ab)	Average of Molecules A and B	0.1	0.16	0.082	0.052	NA	0.022	0.021	0.027	0.028
s3-Form I	Residue	E868	E868	E870	H_2O		T891	D897	D899	D899
	Atom	OE1	OE2	OE2	O	Ca^{2+}	O	OD2	OD1	OD2
Oxygen-calcium distances (Å)	Average of Molecules A, B and C	2.64 (10)	2.46 (7)	2.26 (4)	2.41 (5)	3.77 (2)	2.29 (6)	2.50 (1)	2.54 (5)	2.52 (3)
Distance out of square LSQ plane (Å) (ab)	Average of Molecules A, B and C	0.045 (3)	0.046 (4)	0.034 (2)	0.035 (3)	NA	0.21 (11)	0.17 (7)	0.25 (10)	0.23 (11)
s3-Form II	Residue	E868	E868	E870	H_2O		T891	D897	D899	D899
	Atom	OE1	OE2	OE2	O		O	OD2	OD1	OD2
Oxygen-calcium distances (Å)	Average of Molecules A, B and C	2.57 (13)	2.49 (6)	2.36 (8)	2.78	3.66 (15)	2.25 (11)	2.34 (3)	2.41 (7)	2.41 (1)

The two planar faces are listed separately. Measurements are for the distance of specific atom out of the plane created the four members of each face. Again, a number within parenthesis represents the standard deviation obtained after least square refinement.

Supplementary Table 4. Deviation from planarity in square antiprismatic coordination found in proteins.

Protein	s3b	s3	2AAA	3TEC	2PRK	1JPQ	1K4C
Resolution (Å)	1.4	2.0	2.1	2.0	1.5	1.6	2.0
Ion	Ca^{2+}	Ca^{2+}	Ca^{2+}	Ca^{2+}	Ca^{2+}	K^{+}	K^{+}
Average planar deviation (Å)	0.08	0.01	0.14	0.12	0.01	0.02	0.00
Average ion-to-ligand distance (Å)	2.58	2.45	2.59	2.45	2.48	2.78	2.83

PDB access codes are for proteinase K (2PRK), alpha amylase (2AAA), thermitase (3TEC), G-quadruplex (1JPQ), and KcsA potassium channel (1K4C). The planes for 1K4C are defined by crystallographic symmetry.

Supplementary Table 5: Stability information of *apo* and *holo* s3

	Apo-s3			*Holo*-s3		
Parameters	Heat	Urea	GuHCl	Heat	Urea	GuHCl
ΔG_{HOH} (kcal*mol^{-1})	5.2	1.7	1.8	NA	9.6	8.1
m (kcal*mol^{-1}*M^{-1})	0.1	0.6	2.3	NA	1.5	4.2
C_M (M)	NA	2.7	0.8	NA	6.5	1.9
T_M (°C)	70.2[a] 64.6[b]	NA	NA	94.1[a] >100[b]	NA	NA

(a) Value represents T_M for DSC data shown in Fig-5.

(b) Value represents T_M for denaturation curve shown in Fig-6A

Supplementary Table 6: Conserved water mediated hydrogen-bonds in s3 and s3b.

HOH mediated H-bonds in s3b	HOH mediated H bonds in s3
K908_O...HOH...T910_OG1	T877_O...HOH...S87_OG1
K900_O...HOH...T910_OG1	K869_O...HOH...S87_OG1
K908_O...HOH...N902_O	T877_O...HOH...P87_O
A909_O…HOH…K900_O	A878_O…HOH...K86_O

K908_O…HOH…T910_OG1 indicates that a water molecule is found between carbonyl oxygen of K908 and side-chain alcohol group of T910.

Supplementary Table 7: Data collection statistics for s3b.

Shell low limit	Shell high limit	data completeness	average redundancies	I/σI	R_{sym} (a)
16.61	2.91	98.8	4.8	53.1	2.8
2.91	2.31	100	4.9	34.2	4.3
2.31	2.02	100	4.9	25.7	5.7
2.02	1.83	100	4.9	17.8	8.7
1.83	1.70	100	4.8	12.0	14.1
1.70	1.60	100	4.8	8.1	22.0
1.60	1.52	100	4.7	5.8	30.8
1.52	1.45	100	4.6	3.9	43.6
1.45	1.40	100	4.1	2.6	57.3
1.40	1.35	99.4	3.2	1.8	65.5
all hkl		99.8	4.6	26.3	5.7

(a) $R_{sym} = \sum_h \sum_l |I_{hl} - \langle I_h \rangle| / \sum_h \sum_l \langle I_h \rangle$

Supplementary Table 8: Data collection statistics for s3-Form I.

Shell low limit	Shell high limit	Data completeness	Average redundancies	I/σI	R_{sym}
28.50	5.42	96.6	3.9	37.7	2.4
5.42	4.31	97.6	4.0	37.4	2.7
4.31	3.76	98.8	3.9	33.2	4.1
3.76	3.42	98.9	4.0	30.2	5.9
3.42	3.17	99.4	4.0	24.0	7.5
3.17	2.99	99.5	4.1	19.6	8.6
2.99	2.84	99.5	4.0	15.0	10.3
2.84	2.71	99.5	4.1	12.2	12.2
2.71	2.61	99.6	4.1	10.1	14.6
2.61	2.52	99.7	4.1	9.0	16.7
2.52	2.44	99.8	4.1	8.0	18.0
2.44	2.37	99.8	4.1	6.6	22.6
2.37	2.31	100.0	4.1	6.2	24.5
2.31	2.25	99.8	4.1	5.9	25.7
2.25	2.2	99.9	4.1	5.6	28.2
2.20	2.15	100.0	4.1	4.7	31.8
2.15	2.11	100.0	4.1	3.9	39.6
2.11	2.07	100.0	4.1	3.7	40.9
2.07	2.03	99.9	4.1	3.4	44.8
2.03	2.00	99.9	4.1	3.1	49.2
All hkl		99.4	4.0	16.7	8.6

Supplementary Table 9: Data collection statistics for s3-Form II.

Shell low limit	Shell high limit	Data completeness	Average redundancies	I/σI	R_{sym}
28.68	5.96	93.3	3.5	27.5	4.3
5.96	4.73	96.7	3.5	25.0	5.1
4.73	4.14	97.0	3.5	24.4	6.3
4.14	3.76	97.6	3.5	20.8	7.9
3.76	3.49	97.8	3.6	19.5	9.4
3.49	3.29	98.7	3.6	14.9	11.1
3.29	3.12	99.3	3.6	12.2	12.8
3.12	2.99	99.4	3.6	9.5	15.6
2.99	2.87	99.5	3.6	7.6	18.9
2.87	2.77	99.4	3.6	5.9	23.5
2.77	2.68	99.9	3.6	4.7	30.6
2.68	2.61	99.8	3.6	4.3	32.5
2.61	2.54	99.8	3.6	3.6	36.2
2.54	2.48	100.0	3.6	3.4	43.5
2.48	2.42	100.0	3.6	3.0	45.1
2.42	2.37	99.9	3.6	2.8	50.3
2.37	2.32	99.8	3.5	2.6	52.1
2.32	2.28	99.8	3.5	2.8	52.3
2.28	2.24	99.8	3.4	2.4	52.9
2.24	2.20	99.7	3.4	2.4	55.8
All hkl		98.8	3.6	9.6	15.2

Figures

Supplementary Figure – 1

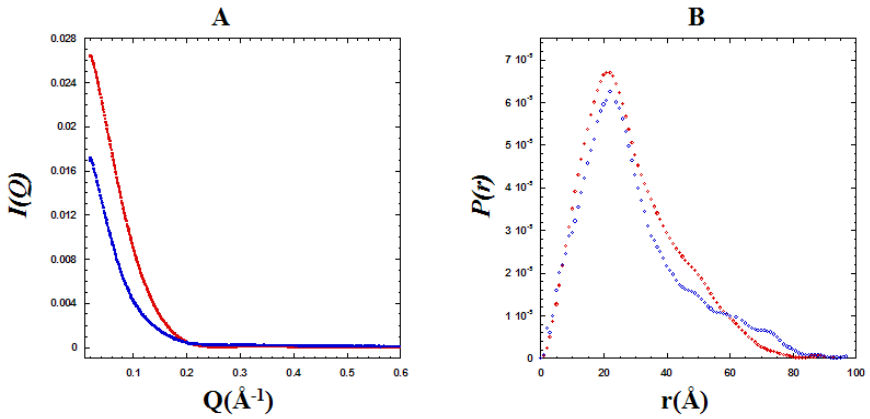

SAXS data of s3-$[G(POG)_8]_3$ complex (blue) and s3b-$[G(POG)_7PRG]_3$ complex (red). (A) The scattering profile where the intensity, *I(Q)* is plotted against scattering vector Q. (B) Pair-distance distribution function *P(r)* in the real space obtained using GNOM.

Supplementary Figure – 2

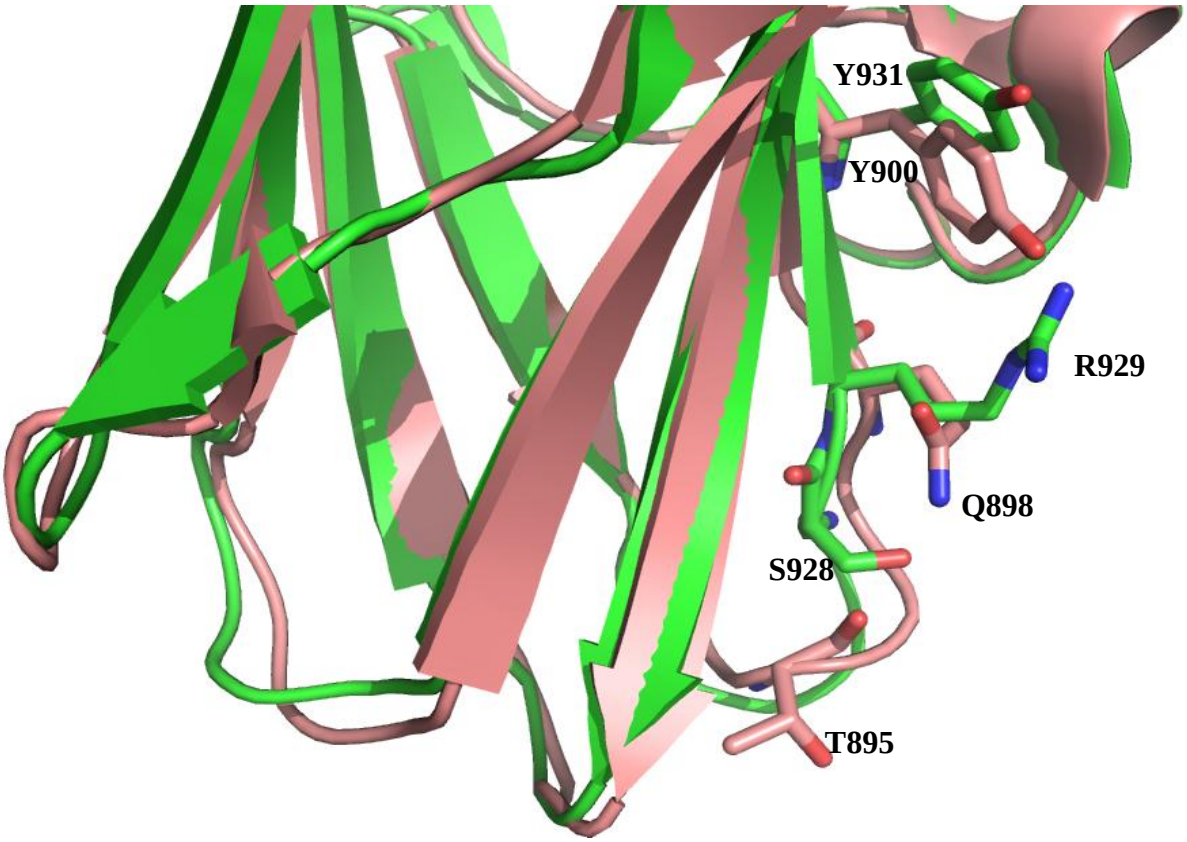

Superimposed structure of s3 (salmon) and s3b (green), showing that Y900 of s3 occupies three dimensional space of R929 of s3b and that T895 of s3 occupies three dimensional space of S928 of s3b.

Supplementary Figure – 3

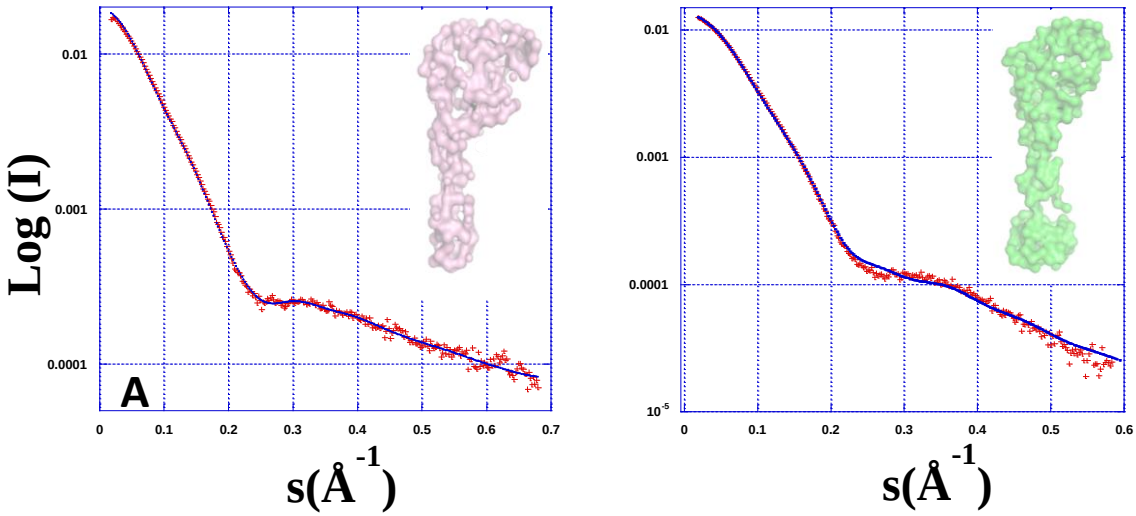

SAXS curves of s3-$[G(POG)_8]_3$ complex (A) and s3b-$[G(POG)_7PRG]_3$ complex (B) are compared to the theoretical scattering durve. The theoretical R_g values calculated from the models by using CRYSOL are in excellent agreement with the experiemental curves (Table-2). Rigid body model with lowest χ value for s3-$[G(POG)_8]_3$ complex (A) and s3b-$[G(POG)_7PRG]_3$ complex (B) are also shown.